J|A|C|S
ARTICLES
Published on Web 03/31/2007

Single-Wall Carbon Nanotubes Bearing Covalently Linked Phthalocyanines − Photoinduced Electron Transfer

Beatriz Ballesteros,[†] Gema de la Torre,[†] Christian Ehli,[‡] G. M. Aminur Rahman,[‡] F. Agulló-Rueda,[§] Dirk M. Guldi,*[,‡] and Tomás Torres*[,†]

Contribution from the Departamento de Química Orgánica, Universidad Autónoma de Madrid, Cantoblanco 28049-Madrid, Spain, University of Erlangen, Institute of Physical and Theoretical Chemistry and Interdisciplinary Center for Molecular Materials, Egerlandstrasse 3, 91058 Erlangen, Germany, and Instituto de Ciencia de Materiales de Madrid, CSIC, Cantoblanco 28049-Madrid, Spain

Received November 17, 2006; E-mail: tomas.torres@uam.es; guldi@chemie.uni-erlangen.de

Abstract: HiPco single-walled carbon nanotubes (SWNTs) have been sidewall-functionalized with phthalocyanine addends following two different approaches: a straightforward Prato reaction with *N*-octylglycine and a formyl-containing phthalocyanine, and a stepwise approach that involves a former Prato cycloaddition to the double bonds of SWNTs using *p*-formyl benzoic acid followed by esterification of the derivatized nanotubes with an appropriate phthalocyanine molecule. The two materials obtained by these routes comprise different carbon/Pc-addenda ratios, as evidenced by Raman, TGA, and photophysical studies. The occurrence of electron transfer from photoexcited phthalocyanines to the nanotube framework in these ZnPc-SWNT ensembles is observed in transient absorption experiments, which confirm the absorption of the one-electron oxidized ZnPc cation and the concomitant bleaching of the van Hove singularities typical from SWNTs. Charge-separation (i.e., 2.0×10^{10} s^{-1}) and charge-recombination (i.e., 1.5×10^{6} s^{-1}) dynamics reveal a notable stabilization of the radical ion pair product in dimethylformamide.

Introduction

The outstanding properties of single-walled carbon nanotubes (SWNTs) have aroused tremendous interest to implement this novel carbon allotrope into practical applications such as molecular electronics, gas storage, sensing, field-emission, etc.[1] Ultimately, attention has even been directed to prepare electron-donor−acceptor nanohybrids/nanoconjugates that are built on carbon nanotubes (CNT).[2] Hereby, the covalent attachment of electron donors that range from pyrene[3] and ferrocene[4] to tetrathiafulvalene (TTF)[5] to the nanotube surface is at the forefront of investigations. Implicit in this concept is that SWNTs accept electrons with ease, which, in turn, might be transported under nearly ballistic conditions along the tubular axis.

Functionalizing CNT with electron-donor antenna chromophores is expected to lead to the development of novel nanoconjugate systems that bear great promise for major breakthroughs in converting solar energy into electricity.[6,7] Thus, the combination of a light-harvester/electron-donor molecule, like porphyrins, together with an electron acceptor, the all-carbon framework of CNT, might lead to highly efficient photovoltaic cells. Recently, it was shown that examples of covalent[8] and, to a similar extent, noncovalent[9,10] porphyrin-SWNT nanoassemblies exhibit, in fact, the much anticipated electron-transfer properties.

Phthalocyanine−nanotube hybrids also emerged as effective targets for photovoltaic devices. Phthalocyanines (Pcs)[11,12] are planar electron-rich aromatic macrocycles that are characterized by their remarkably high extinction coefficients in the red/near-infrared region, an important part of the solar spectrum, and their outstanding photostability and singular physical properties.[13] These features render them exceptional donor/antenna

[†] Universidad Autónoma de Madrid.
[‡] Universität Erlangen.
[§] Instituto de Ciencia de Materiales de Madrid.

(1) *Carbon Nanotubes: Synthesis, Structure, Properties and Applications*; Dresselhaus, M. S., Dresselhaus, G., Avouris, P., Eds.; Springer: Berlin, 2001.
(2) Guldi, D. M.; Rahman, G. M. A.; Zerbetto, F.; Prato, M. *Acc. Chem. Res.* **2005**, *38*, 871.
(3) (a) Georgakilas, V.; Kordatos, K.; Prato, M.; Guldi, D. M.; Holzinger, M.; Hirsch, A. *J. Am. Chem. Soc.* **2002**, *124*, 760. (b) Qu, L.; Martin, R. B.; Huang, W.; Fu, K.; Zweifel, D.; Lin, Y.; Sun, Y.-P. Bunker, C. E.; Harruff, B. A.; Gord, J. R.; Allard, L. F. *J. Chem. Phys.* **2002**, *117*, 8089. (c) Martin, R. B.; Qu, L.; Lin, Y.; Harruff, B. A.; Bunker, C. E.; Gord, J. R.; Allard, L. F.; Sun, Y.-P. *J. Phys. Chem. B* **2004**, *108*, 11447. (d) Alvaro, M.; Atienzar, P.; Bourdelande, J. L.; García, H. *Chem. Phys. Lett.* **2004**, *384*, 119.
(4) (a) Guldi, D. M.; Marcaccio, M.; Paolucci, D.; Paolucci, F.; Tagmatarchis, N.; Tasis, D.; Vázquez, E.; Prato, M. *Angew. Chem., Int. Ed.* **2003**, *42*, 4206. (b) Yang, X.; Lu, Y.; Ma, Y.; Li, Y.; Du, F.; Chen, Y. *Chem. Phys. Lett.* **2006**, *420*, 416.
(5) Herranz, M. A.; Martin, N.; Campidelli, S.; Prato, M.; Brehm, G.; Guldi, D. M. *Angew. Chem., Int. Ed.* **2006**, *45*, 4478.
(6) (a) Barazouk, S.; Hotchandani, S.; Vinodgopal, K.; Kamat, P. V. *J. Phys. Chem. B* **2004**, *108*, 17015. (b) Bhattacharyya, S.; Kymakis, E.; Amaratunga, G. A. J. *Chem. Mater.* **2004**, *16*, 4819. (c) Robel, I.; Bunker, B. A.; Kamat, P. V. *Adv. Mater.* **2005**, *17*, 2458.
(7) Rahman, G. M. A.; Guldi, D. M.; Cagnoli, R.; Mucci, A.; Schenetti, L.; Vaccari, L.; Prato, M. *J. Am. Chem. Soc.* **2005**, *127*, 10051.
(8) (a) Guldi, D. M.; Rahman, G. M. A.; Ramey, J.; Marcaccio, M.; Paolucci, D.; Paolucci, F.; Qin, S.; Ford, W. T.; Balbinot, D.; Jux, N.; Tagmatarchis, N.; Prato, M. *Chem. Commun.* **2004**, 2034. (b) Guldi, D. M.; Rahman, G. M. A.; Prato, M.; Jux, N.; Qin, S.; Ford, W. *Angew. Chem., Int. Ed.* **2005**, *44*, 2015. (c) Guldi, D. M.; Rahman, G. M. A.; Qin, S.; Tchoul, M.; Ford, W. T.; Marcaccio, M.; Paolucci, D.; Paolucci, F.; Campidelli, S.; Prato, M. *Chem.-Eur. J.* **2006**, *12*, 2152.

building blocks. Incorporating them into donor−acceptor systems together with, for example, fullerenes,[14−16] perylenes,[17] anthraquinones,[18] or related metallomacrocycles[19] gives rise to long-lived and highly emissive charge-separated states. In this context, we have recently demonstrated that anchoring a novel titanium phthalocyanine to nanocrystalline TiO_2 films affords electron injection from the titanium phthalocyanine to the TiO_2.[20]

Some previous work has reported on the preparation of CNT-phthalocyanine composites[21] or nanowires.[22] These hybrid materials show enhanced photoconductivity, as a result of photoinduced charge transfer from the Pc excitons to CNT. On the other hand, covalent functionalization of carbon nanotubes with Pc moieties has also been reported by us[23] and others[24,25] through a reaction of the terminal carboxylic acid groups of shortened chemically etched SWNT with amino-functionalized phthalocyanines. However, the resulting materials proved to be nearly insoluble in common organic solvents. The solubility/dispersability of Pc-CNT material emerged as an indispensable task to be resolved for a ready manipulation and a feasible solution-phase processing of such nanohybrids into devices. Moreover, most of the important photophysical analyses (i.e., identifying promising hybrids/conjugates for solar energy conversion) are performed in condensed media.

The development of chemical strategies, aimed at solubilizing SWNT, has lately driven the research in this area.[26] In particular, organic covalent functionalization at the sidewalls of carbon nanotubes usually leads to very soluble materials.[27,28] Derivatization based on 1,3-dipolar cycloaddition of azomethine ylides, generated by condensation of α-aminoacids and aldehydes, has been shown to be a powerful methodology for functionalizing and solubilizing CNT.[26,29] This widely applicable approach affords functionalized SWNT, in which the tubular structure is preserved. Moreover, they are soluble enough to facilitate manipulation and solution studies.

In the current work, we report on the preparation of new dispersable ZnPc-SWNT hybrids through the Prato reaction of HiPco SWNT, *N*-octylglycine, and adequately functionalized ZnPc molecules, bearing six solubilizing groups and an aldehyde. Alternatively, a stepwise approach has been explored to achieve a high degree of CNT functionalization at minimum synthetic costs. Importantly, we complement our work with a detailed photophysical investigation on ground- and excited-state Pc−nanotube interactions.

Results and Discussion

In general, two possible routes toward functionalizing SWNT with ZnPc, see Scheme 1, could be considered, both following the Prato protocol. The first route (route 1, Scheme 1) would involve the former reaction of *N*-octylglycine[30] and 4-formylbenzoic acid with SWNTs and subsequent esterification reaction of the derivatized nanotube material with 2,3,9,10,16,17-hexa-*tert*-butylphenoxy-2-hydroxymethylphthalocyaninate Zn(II) (**1**), see Scheme 2. This approach is fairly advantageous, because, as previously described,[27−29] chemical modification of CNT usually requires a large excess of the reactants. In this particular case, one of them is the inexpensive 4-formylbenzoic acid. Subsequent esterification reaction of the pyrrolidine-SWNT bearing pendent COOH moieties and zinc(II) phthalocyanine **1** would proceed at nearly stoichiometric conditions (Scheme 1).

Pthalocyanine **1** was prepared by condensation of 4,5-*tert*-butylphenoxyphthalonitrile[31] and 4-hydroxymethylphthalonitrile[18] in the presence of $Zn(OAc)_2$ in 11% yield (Scheme 2). The compound was characterized by standard spectroscopic techniques. It is worth pointing out that the room-temperature ^{1}H-NMR spectrum of this compound reveals an unusual shielding of some of the aromatic signals (ca. 6.5 ppm in $CDCl_3$, 6.9 in $C_2D_4Cl_4$). In particular, those are affected that correspond to the hydroxymethyl-containing isoindole units of the Pc core, while the remaining aromatic protons appear at average chemical

(9) (a) Baskaran, D.; Mays, J. W.; Zhang, X. P.; Bratcher, M. S. *J. Am. Chem. Soc.* **2005**, *127*, 6916. (b) Alvaro, M.; Atienzar, P.; de la Cruz, P.; Delgado, J. L.; Troiani, V.; García, H.; Langa, F.; Palkar, A.; Echegoyen, L. *J. Am. Chem. Soc.* **2006**, *128*, 6626. (c) Murakami, H.; Nomura, T.; Nakashima, N. *Chem. Phys. Lett.* **2003**, *378*, 481. (d) Tanaka, H.; Yajima, T.; Matsumoto, T.; Otsuka, Y.; Ogawa, T. *Adv. Mater.* **2006**, *18*, 1411. (e) Hecht, D. S.; Ramirez, R. J. A.; Briman, M.; Artukovic, E.; Chichak, K. S.; Stoddart, J. F.; Gruner, G. *Nano Lett.* **2006**, *6*, 2031. (f) Cheng, F.; Adronov, A. *Chem.-Eur. J.* **2006**, *12*, 5053.

(10) (a) Guldi, D. M.; Rahman, G. M. A.; Jux, N.; Tagmatarchis, N.; Prato, M. *Angew. Chem., Int. Ed.* **2004**, *43*, 5526. (b) Guldi, D. M.; Taieb, H.; Rahman, G. M. A.; Tagmatarchis, N.; Prato, M. *Adv. Mater.* **2005**, *17*, 871. (c) Ehli, C.; Rahman, G. M. A.; Jux, N.; Balbinot, B.; Guldi, D. M.; Paolucci, F.; Marcaccio, M.; Melle-Franco, M.; Zerbetto, F.; Campidelli, S.; Prato, M. *J. Am. Chem. Soc.* **2006**, *128*, 11222.

(11) (a) *Phthalocyanines: Properties and Aplications*; Leznoff, C. C., Lever, A. B. P., Eds.; VCH: Weinheim, 1989, 1993, 1996; Vols. 1−4. (b) *The Porphyrin Handbook*; Kadish, K. M., Smith, K. M., Guilard, R., Eds.; Academic Press: San Diego, CA, 2003; Vols. 15−20.

(12) McKeown, N. B. *Phthalocyanine Materials: Synthesis, Structure and Function*; Cambridge University Press: Cambridge, 1998.

(13) (a) de la Torre, G.; Vázquez, P.; Agulló-López, F.; Torres, T. *Chem. Rev.* **2004**, *104*, 3723. (b) de la Torre, G.; Claessens, C. G.; Torres, T. *Chem. Commun.*, in press.

(14) (a) Guldi, D. M.; Gouloumis, A.; Vázquez, P.; Torres, T. *Chem. Commun.* **2002**, 2056. (b) Loi, M. A.; Neugebauer, H.; Denk, P.; Brabec, C. J.; Sariciftci, N. S.; Gouloumis, A.; Vázquez, P.; Torres, T. *J. Mater. Chem.* **2003**, *13*, 700. (c) Guldi, D. M.; Zilbermann, I.; Gouloumis, A.; Vázquez, P.; Torres, T. *J. Phys. Chem. B* **2004**, *108*, 18485. (d) Gouloumis, A.; de la Escosura, A.; Vázquez, P.; Torres, T.; Kahnt, A.; Guldi, D. M.; Neugebauer, H.; Winder, C.; Drees, M.; Sariciftci, N. S. *Org. Lett.* **2006**, *8*, 5187.

(15) Guldi, D. M.; Gouloumis, A.; Vázquez, P.; Torres, T.; Georgalikas, V.; Prato, M. *J. Am. Chem. Soc.* **2005**, *127*, 5811.

(16) (a) de la Escosura, A.; Martínez-Díaz, M. V.; Guldi, D. M.; Torres, T. *J. Am. Chem. Soc.* **2006**, *128*, 4112. (b) Guldi, D. M.; Ramey, J.; Martínez-Díaz, M. V.; de la Escosura, A.; Torres, T.; Da Ros, T.; Prato, M. *Chem. Commun.* **2002**, 2774. (c) Ballesteros, B.; de la Torre, G.; Hug, G. L.; Rahman, G. M. A.; Guldi, D. M. *Tetrahedron* **2006**, *62*, 2097. (d) Torres, T.; Gouloumis, A.; Sanchez-García, D.; Jayawickramarajah, J.; Seitz, W.; Guldi, D. M.; Sessler, J. L. *Chem. Commun.* **2007**, 292.

(17) Rodríguez-Morgade, M. S.; Torres, T.; Atienza-Castellanos, C.; Guldi, D. M. *J. Am. Chem. Soc.* **2006**, *128*, 15145.

(18) Gouloumis, A.; Gonzalez-Rodriguez, D.; Vazquez, P.; Torres, T.; Liu, S.; Echegoyen, L.; Ramey, J.; Hug, G. L.; Guldi, D. M. *J. Am. Chem. Soc.* **2006**, *128*, 12674.

(19) (a) González-Rodríguez, D.; Claessens, C. G.; Torres, T.; Liu, S.-G.; Echegoyen, L.; Vila, N.; Novell, S. *Chem.-Eur. J.* **2005**, *11*, 3881. (b) Claessens, C. G.; Torres, T. *Angew. Chem., Int. Ed.* **2002**, *41*, 2561. (c) Claessens, C. G.; Torres, T. *J. Am. Chem. Soc.* **2002**, *124*, 14522. (d) García-Frutos, E. M.; Fernández-Lázaro, F.; Maya, E. M.; Vázquez, P.; Torres, T. *J. Org. Chem.* **2000**, *65*, 6841.

(20) Palomares, E.; Martínez-Díaz, M. V.; Haque, S. A.; Torres, T.; Durrant, J. R. *Chem. Commun.* **2004**, 2112.

(21) Cao, L.; Chen, H.; Wang, M.; Sun, J.; Zhang, X.; Kong, F. *J. Phys. Chem. B* **2002**, *106*, 8971.

(22) Cao, L.; Chen, H.-Z.; Zhou, H.-B.; Zhu, L.; Sun, J.-Z.; Zhang, X.-B.; Xu, J.-M.; Wang, M. *Adv. Mater.* **2003**, *15*, 909.

(23) de la Torre, G.; Blau, W.; Torres, T. *Nanotechnology* **2003**, *14*, 765.

(24) Yang, Z.-L.; Chen, H.-Z.; Cao, L.; Li, H.-Y.; Wang, M. *Mater. Sci. Eng., B* **2004**, *106*, 73.

(25) Xu, H.-B.; Chen, H.-Z.; Shi, M.-M.; Bai, R.; Wang, M. *Mater. Chem. Phys.* **2005**, *94*, 342.

(26) Tasis, D.; Tagmatarchis, N.; Georgakilas, V.; Prato, M. *Chem.-Eur. J.* **2003**, *9*, 4001.

(27) (a) Hirsch, A. *Angew. Chem., Int. Ed.* **2002**, *41*, 1853. (b) Niyogi, S.; Hamon, M. A.; Hu, H.; Zhao, B.; Bhowmik, P.; Sen, R.; Itkis, M. E.; Haddon, R. C. *Acc. Chem. Res.* **2002**, *35*, 1105. (c) Dyke, C. A.; Tour, J. M. *J. Phys. Chem. A* **2004**, *51*, 11151.

(28) (a) Banerjee, S.; Hemraj-Benny, T.; Wong, S. S. *Adv. Mater.* **2005**, *17*, 17. (b) Hirsch, A.; Vostrowsky, O. *Top. Curr. Chem.* **2005**, *245*, 193. (c) Tasis, D.; Tagmatarchis, N.; Bianco, A.; Prato, M. *Chem. Rev.* **2006**, *106*, 1105.

(29) Georgakilas, V.; Kordatos, K.; Prato, M.; Guldi, D. M.; Holzinger, M.; Hirsch, A. *J. Am. Chem. Soc.* **2002**, *124*, 760.

(30) Segura, M.; Sánchez, L.; de Mendoza, J.; Martín, N.; Guldi, D. M. *J. Am. Chem. Soc.* **2003**, *125*, 15093.

(31) Maree, S. E.; Nyokong, T. *J. Porphyrins Phthalocyanines* **2001**, *5*, 782.

Scheme 1. Chemical Routes Followed To Functionalize the Sidewalls of SWNTs with Pc Molecules: Preparation of **ZnPc-SWNT-(1)** and **ZnPc-SWNT-(2)**

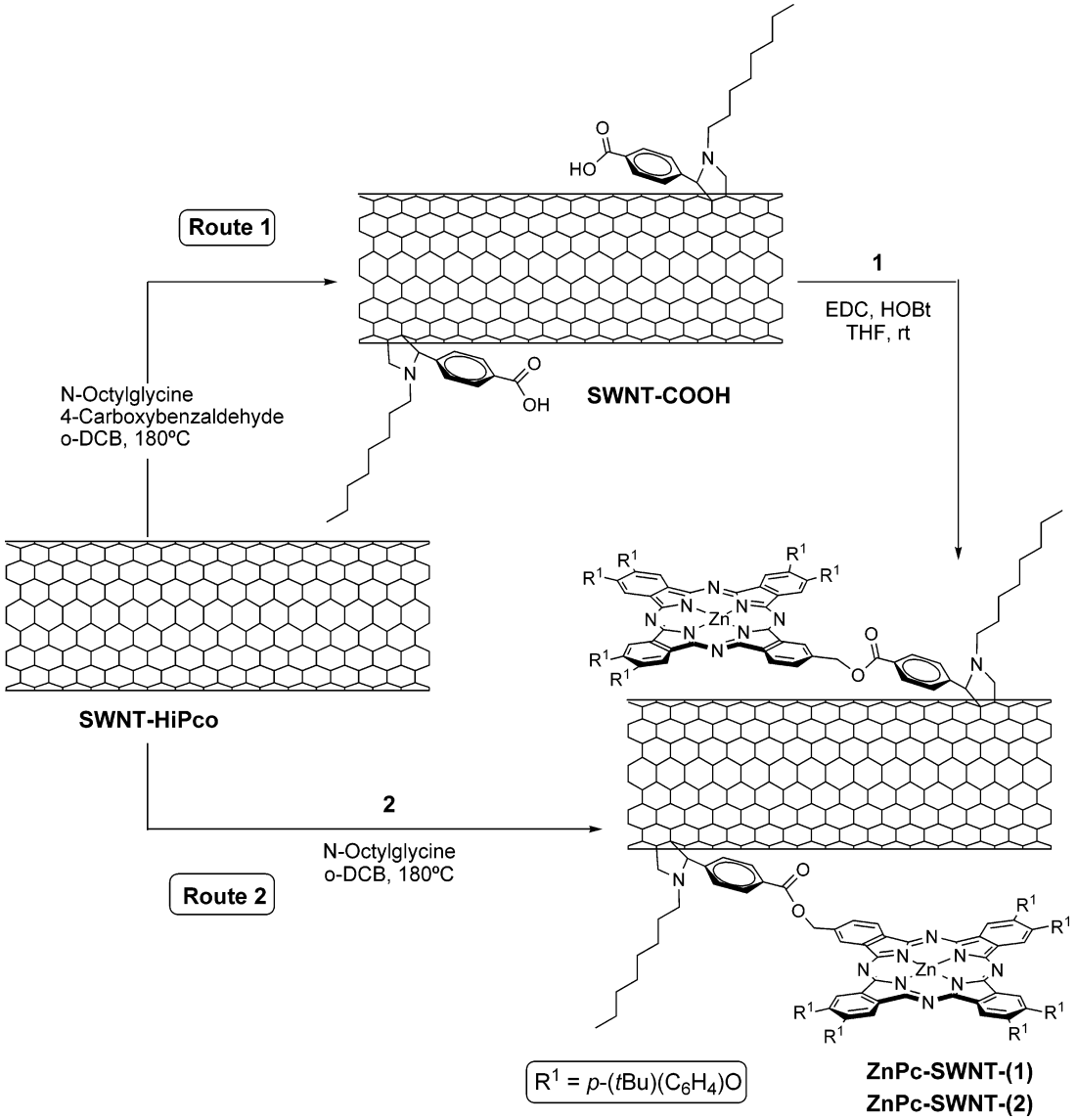

shifts (8−9 ppm). However, when the experiments are carried out at higher temperatures (i.e., 60 °C), the signal at 6.8 ppm in deuterated tetrachloroethane decreases and a new signal centered at 7.7 ppm grows-in. At 90 °C, the former signal has fully disappeared. A likely rationale for this behavior stems from possible aggregations between individual Pc, mainly through coordination between the CH_2OH groups and the Zn centers.[32]

We performed the modification of the nanotube sidewalls (Scheme 1) using, as previously described, 1.2 equiv of *N*-octylglycine and 4-formylbenzoic acid per carbon atom of the nanotube structure. In our hands, refluxing *o*-dichlorobenzene instead of DMF at 130 °C[29] affords larger amounts of functionalized **COOH-SWNT** material. Clear evidence of the introduction of COOH moieties in the material comes from the IR spectrum (see below). The concentration of pyrrolidine-COOH moieties in the SWNT was estimated to be ca. 7% by acid−base titration[33] (see Experimental Section). This derivatized SWNT material was reacted with an excess (ca. 3 equiv) of phthalocyanine **1** in THF/DMF dispersions in the presence of the EDC/HOBT condensation mixture (Scheme 1). After 4 days of reaction, the ZnPc-SWNT hybrid material (**ZnPc-SWNT-(1)**) was filtered through a PTFE membrane and washed with several solvents.

A set-back of this route lies in the fact that it is very difficult to control the number of −COOH moieties that are subject to esterification with phthalocyanines. For this reason, we explored a second strategy (route 2, Scheme 1), that is, preparing a formyl-containing phthalocyanine **2** (Scheme 2). The benefit of this strategy is that a formyl-containing phthalocyanine **2** is straightforwardly attached to CNT through the formation of the corresponding azomethine ylide. In this case, the esterification reaction of phthalocyanine **1** and 4-formylbenzoic acid using standard condensation conditions leads to phthalocyanine **2** in 93% yield (Scheme 2). In the reaction with 4-formylbenzoic acid and SWNTs, we observed a large amount of degraded

(32) (a) Senge, M. O.; Speck, M.; Wiehe, A.; Dieks, H.; Aguirre, S.; Kurreck, H. *Photochem. Photobiol.* **1999**, *70*, 206. (b) Teo, T.-L.; Vetrichelvan, M.; Lai, Y.-H. *Org. Lett.* **2003**, *5*, 4207.

(33) Hu, H.; Bhowmik, P.; Zhao, B.; Hamon, M. A.; Itkis, M. E.; Haddon, R. C. *Chem. Phys. Lett.* **2001**, *345*, 25.

Scheme 2. Synthesis of Phthalocyanines **1** and **2**

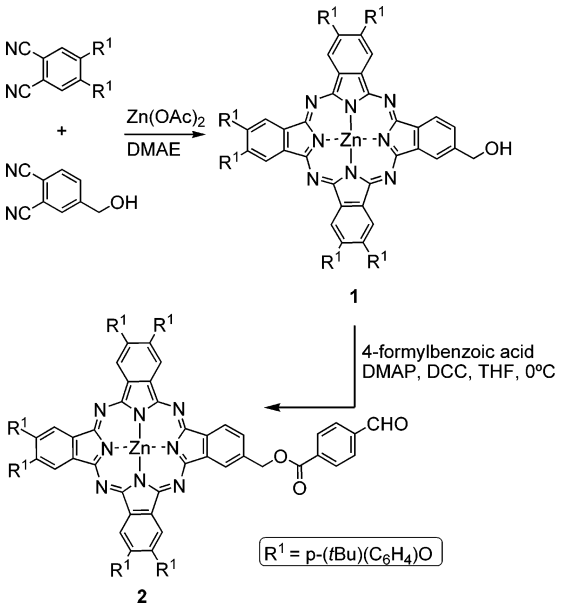

material arising from the organic reactants. Therefore, considering that formyl-Pc **2** is a highly elaborated compound, we decided to employ a lower excess of **2**. Thus, we used 1 equiv of Pc **2** every 25 carbon atoms for the 1,3-dipolar cycloaddition with SWNT. After 5 days of reaction, the green color fully disappeared and a dark-brownish mixture was instead present. The functionalized nanotube material **ZnPc-SWNT-(2)** was filtered off and accordingly washed with several organic solvents.

Chemically modified **ZnPc-SWNT-(1)** and **ZnPc-SWNT-(2)** form stable dispersions in DMF. Both materials were characterized by analytical and spectroscopic methods: all data are consistent with a successful functionalization of SWNT with Pc molecules.

Representative TEM images of SWNT material are shown in Figure 1. Pristine SWNTs, as received from CNI (Figure 1a), are typically aggregated in bundles, and the presence of metallic (iron) nanoparticles is revealed as black spots. Images of **ZnPc-SWNT-(1)** and **ZnPc-SWNT-(2)** (Figure 1b and c, respectively) reveal less bundled materials than what is typically found for pristine SWNTs. This observation is consistent with SWNT functionalization with phthalocyanines, where Pc rings may disrupt the strong interactions between individual SWNTs.

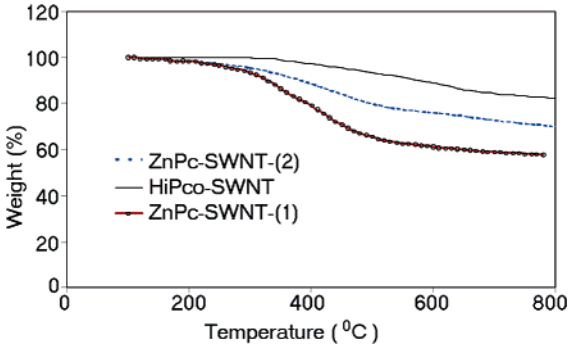

Figure 2. TGA profiles of ZnPc-functionalized SWNT materials and starting HiPco nanotubes. The heating process was carried out under nitrogen.

Additional evidence for the successful functionalization of SWNT is deduced from Raman and IR spectroscopies and thermogravimetric analysis. Figure 2 shows the thermal behavior of the two materials together with that of the starting HiPco-SWNT. The weight loss between 250 and 500 °C is around 30% for **ZnPc-SWNT-(1).** Considering we had ca. a 7% functionalization (from titration, see above) in the starting **COOH-SWNT** material, a 23% weight loss should correspond to the hydroxy-functionalized Pc moiety. Thus, the calculated molar ratio of Pc-pyrrolidine/pyrrolidine-COOH moieties linked to the nanotubes is 1.7, which allows one to estimate that the material still holds a 3% weight of the pyrrolidine-COOH group, and therefore a 27% weight of the Pc-pyrrolydine. Therefore, the Pc-addenda/carbon ratio was calculated to be approximately 1:380. However, the **ZnPc-SWNT-(2)** shows 20% weight loss in TGA, which leads us to conclude that the Pc-addenda/carbon ratio in this material is 1:580. The relatively low functionalization degree of these materials may well be favorable because it preserves the intrinsic electronic properties of nanotubes. It is important to point out that the residue did not decompose up to 800 °C in nitrogen atmosphere. This behavior is consistent with the presence of entire SWNTs in all of the functionalized samples.

Raman spectroscopy provides evidence that functionalization is covalent to the nanotube sidewalls. Figure 3 shows the Raman spectra for the pristine sample (SWNT) and for the phthalocyanine-funtionalized samples **ZnPc-SWNT-(1)** and **ZnPc-SWNT-(2)**. The fluorescence background increases according to the degree of functionalization, partially due to enhancement of Pc-related fluorescence. The Raman spectra are characteristic

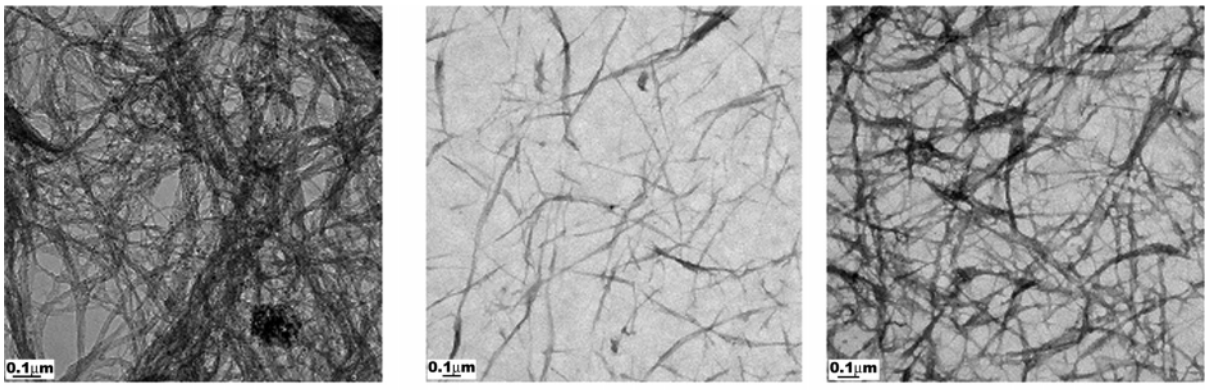

Figure 1. TEM images (on carbon-coated grids) of (a) HiPco SWNT (as received from CNI), (b) **ZnPc-SWNT-(1)**, and (c) **ZnPc-SWNT-(2)**.

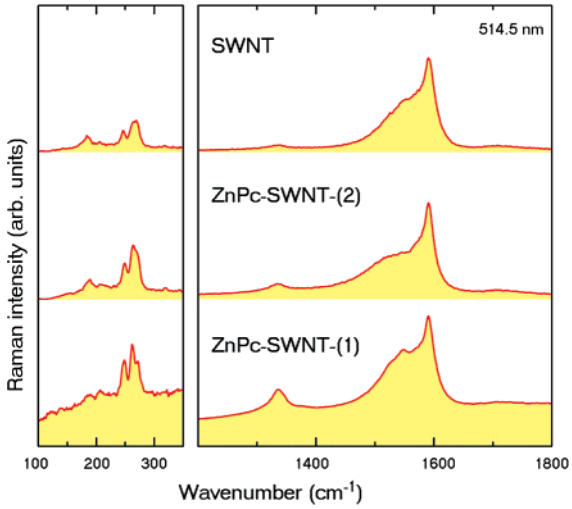

Figure 3. Raman spectra of pristine SWNTs and two nanotube materials functionalized with phthalocyanines: **ZnPc-SWNT-(2)** and **ZnPc-SWNT-(1)**. Spectra have been offset vertically for clarity. The colored area under each spectrum marks the zero level. The intensities on the left panel (RBM peaks) are multiplied approximately by ×5 relative to the right panel (D and G bands).

of single-wall nanotubes, with several radial breathing modes (RBM) between 186 and 270 cm^{-1}, corresponding to nanotube diameters[34] between 0.92 and 1.33 nm, a D band at about 1355 cm^{-1}, due to disorder on the carbon hexagonal lattice on the nanotube sidewalls, and several tangential modes (TM) or G bands between 1400 and 1600 cm^{-1}. We have not found clear evidence of any peak characteristic of the functionalizing moieties, because functionalization is weak. However, functionalization does induce an enhancement of the D band,[35] with respect to the pristine nanotube, the effect being larger for sample **ZnPc-SWNT-(2)**. The enhancement proves that the functionalization is through covalent bonding with the sidewall carbon atoms, which convert some sp^2 bonding into sp^3.[34]

More evidence to support covalent functionalization of SWNTs is found in the IR spectra (Figure 4). Comparing pristine nanotubes with **COOH-SWNT** material, the presence of COOH moieties in the latter is principally confirmed by the occurrence of a strong band at 1715 cm^{-1} corresponding to the symmetric C═O stretching. The phthalocyanine-functionalized nanotube material **ZnPc-SWNT-(1)** displays the same band but at 1728 cm^{-1}. This shift matches the transformation of the COOH moiety of **COOH-SWNT** into an ester function after reaction with the hydroxyphthalocyanine **1**. Finally, the IR spectrum of **ZnPc-SWNT-(1)** also shows other bands that are coincident with those displayed by phthalocyanine **1**. The IR spectrum of **ZnPc-SWNT-(2)** displays bands that are similar to those of **ZnPc-SWNT-(1)**.

Photophysics. When discussing the ground-state absorption of ZnPc-SWNT, we wish to point out two regions of interest: the visible range, where we mainly find the Pc-centered transitions (i.e., Soret- and Q-bands), and the near-infrared range,

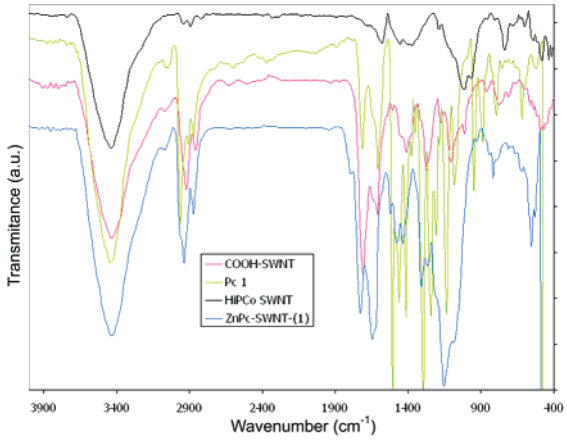

Figure 4. IR spectra of COOH- and Pc-containing nanotubes matched up to those of the starting HiPco material and hydroxymethylphthalocyanine **1**.

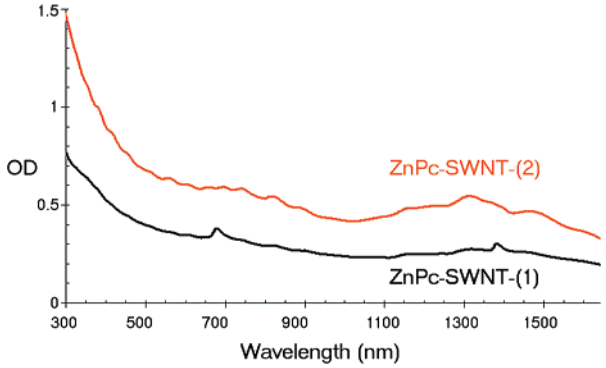

Figure 5. Ground-state absorption spectra of **ZnPc-SWNT-(1)** and **ZnPc-SWNT-(2)** in DMF at room temperature.

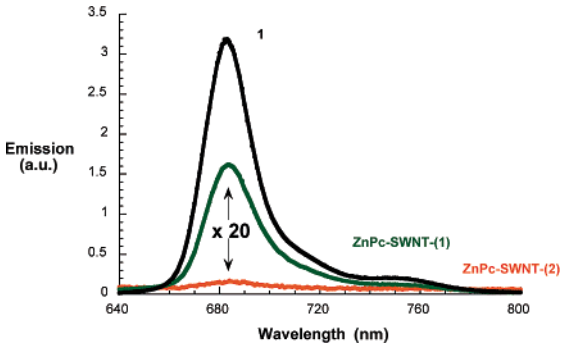

Figure 6. Steady-state fluorescence spectra of **1**, **ZnPc-SWNT-(1)**, and **ZnPc-SWNT-(2)** in DMF at room temperature with matching absorption at the excitation wavelength (i.e., 650 nm). Curves for **ZnPc-SWNT-(1)** and **ZnPc-SWNT-(2)** have been amplified by a factor of 20.

which is dominated by SWNT-related features (i.e., van Hove singularities). At first glance, the ground-state absorption spectra, which reveal the features of both constituents, that is, ZnPc and SWNT, are good mirror reflections of the results that were gathered in the TGA experiments. In particular, depending on the degree of functionalization, that is, comparing **ZnPc-SWNT-(2)** and **ZnPc-SWNT-(1)**, two trends are noteworthy, see Figure 5. First, the overall intensity of the Pc-centered transitions increased from **ZnPc-SWNT-(2)** to **ZnPc-SWNT-(1)**. Second, the SWNT characteristics deintensified concomitantly. Considering the intensity of the 680 nm absorption maximum, we estimate a ZnPc content of around 10% and 20% in **ZnPc-SWNT-(2)** and **ZnPc-SWNT-(1)**, respectively. Nevertheless,

(34) Dresselhaus, M. S.; Dresselhaus, G.; Saito, R.; Jorio, A. *Phys. Rep.* **2005**, *409*, 47.
(35) (a) Chiu, P. W.; Duesberg, G. S.; Hahn, O.; Dettlaff-Weglikowska; Roth, S. *Appl. Phys. Lett.* **2002**, *80*, 3811. (b) Bahr, J. L.; Tour, J. M. *J. Mater. Chem.* **2002**, *12*, 1952. (c) Dyke, C. A.; Tour, J. M. *Chem.-Eur. J.* **2004**, *10*, 812. (d) Marcoux, P. R.; Schreiber, J.; Batail, B.; Lefrant, S.; Renouard, J.; Jacob, G.; Albertini, D.; Mevellec, J.-Y. *Phys. Chem. Chem. Phys.* **2002**, *4*, 2278. (e) Ménard-Moyon, Y. C.; Izard, N.; Doris, E.; Mioskowski, C. *J. Am. Chem. Soc.* **2006**, *128*, 6552.

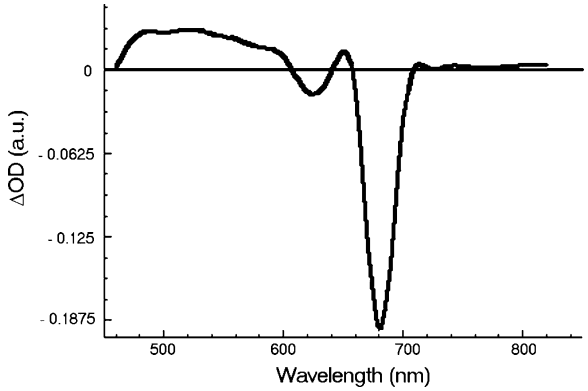

Figure 7. Differential absorption spectrum (visible and near-infrared) obtained upon nanosecond flash photolysis (532 nm) of $\sim 1.0 \times 10^{-5}$ M solutions of **1** in nitrogen-saturated dimethylformamide with a time delay of 50 ns at room temperature. The spectral changes reflect the triplet excited-state features of **1**.

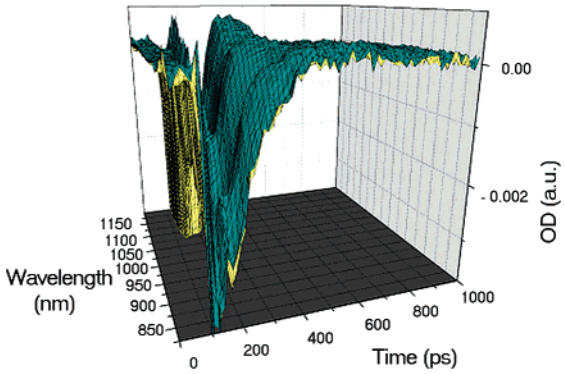

Figure 8. Differential absorption spectrum (near-infrared) obtained upon femtosecond flash photolysis (660 nm) of **ZnPc-SWNT-(2)** in nitrogen-saturated dimethylformamide with time delays between 0 and 1000 ps at room temperature.

a notable red-shift of 2 nm (i.e., 676 to 678 nm) is discernible for ZnPc in the corresponding ZnPc-SWNT conjugates. Such shifts point to some electronic communication between the electroactive components.

More decisive tests about interactions between the ZnPc and SWNT constituents are based on fluorescence experiments, especially considering the prominent ZnPc fluorescence features (i.e., quantum yield, 0.3; lifetime, 3.1 ns). Photoexciting all ZnPc-SWNT conjugates and the ZnPc reference (**1**) in the range of either the Soret- (i.e., $\sim$300−350 nm) or the Q-bands (i.e., 600−680 nm) led to a set of fluorescing features with a strong maximum and a shoulder at 685 and 750 nm, respectively. This confirms unmistakably the presence of the ZnPc constituents in all ZnPc-SWNT samples. Figure 6 demonstrates that a qualitative comparison (i.e., photoexciting around 650 nm) reveals, however, vastly different fluorescence quantum yields. Relative to **1**, the following quenching factors were determined: **ZnPc-SWNT-(2)** (425) and **ZnPc-SWNT-(1)** (40); notably these values have not been corrected for competitive ground-state absorption at the excitation wavelength (vide supra). In reference experiments, where **1** was titrated with variable SWNT concentrations, the lack of appreciable changes suggests no excited-state interactions, see Figure S1.

Not surprising, the corresponding time-resolved fluorescence experiments failed to shed light onto the intraconjugate deactivation of the ZnPc singlet excited state. The time resolution, 100 ps, is mainly thought to be responsible for the lack of detectable ZnPc fluorescence deactivation.

To confirm the aforementioned observations, we turned to femto- (i.e., 660 nm excitation) and nanosecond (i.e., 532 nm excitation) resolved transient absorption spectroscopy. For **1**, which lacks the SWNT, we see the rapid formation of the singlet excited-state characteristics. These include transient bleach in the 600−700 nm range, which mirror images the ground-state absorption (not shown). In addition, in the blue and red regions, new transients are registered. Please note that the one in the blue, at 470 nm, will be of particular importance when testing excited-state interactions in the ZnPc-SWNT conjugates. The fate of the ZnPc singlet excited state is an intersystem crossing ($(3.3 \pm 0.5) \times 10^8$ s^{-1}) that affords the corresponding triplet manifold. An illustration of the triplet spectrum of **1** is given in Figure 7. Please note that in the red region, that is, above 700 nm, no appreciable features are registered for the oxygen-sensitive triplet state.

Initially, upon photoexciting both ZnPc-SWNT conjugates, the ZnPc singlet fingerprints, vide supra, are notable. In the visible range, transient maxima and transient minima centered around 680 and 470 nm, respectively, attest to the successful excitation of the ZnPc constituent in ZnPc-SWNT on the femtosecond time scale. However, instead of the slow intersystem crossings, the singlet excited states decay with rates of about 10^{10} s^{-1} (vide supra), from which we deduce electronic couplings between both electroactive elements of 50 cm^{-1}. Considering approximate absorption cross sections of the ZnPc and SWNT constituents at the 660 nm excitation wavelength in a 1:9 ratio, a significant fraction of the light photoexcites the SWNT. Therefore, we notice the instantaneous bleaching of the van Hove singularities. However, exciton recombination, which depends on the SWNT diameter, leads to rather fast deactivation. Such fast deactivation dynamics are outside of the detection range of our time-resolved fluorescence measurements.

At the end of the intrinsically fast ZnPc singlet excited-state decay, the following differential absorption changes occur for **ZnPc-SWNT-(2)** in the visible and near-infrared regions (Figures 8 and S3 in the Supporting Information); in the visible, its mainly the bleaching of the Q-bands that is appreciable. This is further accompanied by a broad absorption in the 425−575 nm range. In the near-infrared, on the other hand, we see a set of maxima at 840 and 930 nm and a set of minima at 820, 890, 980, 1090, 1150, 1200, and 1310 nm. The maxima, especially the one at 840 nm, are known to reflect the transient spectrum of the one-electron oxidized ZnPc radical cation. The same holds for the 425−575 nm transition. Quite the opposite, the minima relate to the van Hove singularities seen in the ground-state spectrum that bleach upon electron doping. Implicit are new conduction band electrons, injected from photoexcited ZnPc, shifting the transitions to lower energies. Spectroscopic support for this assumption came from determining the absolute spectrum of the product and comparing it with that of the ground state. As Figure S2 illustrates, the van Hove singularities shift indeed to the red. Thus, we reach the conclusion that photoexcitation of ZnPc-SWNT conjugates is followed by a rapid charge transfer. Figures 8 and S3 illustrate the transformation of the ZnPc singlet excited state into the radical ion pair state for **ZnPc-SWNT-(2)** (i.e., 2.0×10^{10} s^{-1}).

Similar changes were noted with **ZnPc-SWNT-(1)**, Figure S4. Important is that the charge-transfer kinetics are virtually identical to the values determined for **ZnPc-SWNT-(2)**.

The decay kinetics, on the nanosecond scale, reflect the return of the radical ion pair state to the electronic ground state. The lifetime of the newly formed radical ion pair state, as derived by analyzing several wavelengths under unimolecular conditions, is, for example, in **ZnPc-SWNT-(2)** 1.5×10^6 s^{-1} in dimethylformamide.

Conclusions

Phthalocyanine-SWNT ensembles have been satisfactorily prepared following the Prato protocol, via 1,3-dipolar cycloaddition of appropriate formyl derivatives with *N*-octylglycine. A straightforward approach and a stepwise one have been explored; the former cycloaddition of a large excess of *p*-formyl benzoic acid (comercial) and the glycine derivative with HiPco SWNT, followed by esterification reaction between the derivatized nanotube material and the hydroxymethylphthalocyanine (**1**), gives a hybrid material (**ZnPc-SWNT-(1)**) largely functionalized (30 wt %), at lower synthetic cost. In addition to that, a second approach has been followed to synthesize **ZnPc-SWNT-(2)** by means of a 1,3-dipolar cycloaddition reaction with phthalocyanine **2**, early containing a formyl group. This route solves the difficulty in controlling the degree of esterification and is presented as a one-step reaction that leads to the same nanohybrid system, developing a lower degree of functionalization (20 wt %). The transient absorption data show that, as previously observed in other donor-SWNT ensembles,[3−5,8−10] SWNTs serve as the electron-acceptor component in such hybrid materials. The estimated number of ZnPc units per carbon atom is quite low (1:380 and 1:580, respectively), which helps, on the other hand, to preserve the electronic structure of SWNTs, as proved by different ground-state and transient absorption spectroscopies. Taken this, together with the light harvesting features of the used phthalocyanines, into concert, our approach toward versatile nanoconjugates opens the way to novel chemical and light driven systems.

Experimental Section

General Methods and Materials. In the experiments, we have used SWNTs prepared by the HiPco process and provided by Carbon Nanotechnologies Inc. The raw material was treated with concentrated HCl to remove the iron content.[36] SWNT derivatives were filtered over 0.45 pore-size PTFE membranes (Sartorius). Chemicals were purchased from commercial suppliers and used without further purification. *N*-Octylglycine,[30] 4,5-*tert*-butylphenoxyphthalonitrile,[31] and 4-hydroxymethylphthalonitrile[18] were prepared using described procedures. Column chromatography was carried out on silica gel Merck-60 (230−400 mesh, 60 Å), and TLC was carried out on aluminum sheets precoated with silica gel 60 F_{254} (E. Merck). PTFE filters (pore size 0.45 μm) were used. Melting points were determined in a Büchi 504392-S equipment and are uncorrected. IR spectra were recorded on a Bruker Vector 22 spectrophotometer using KBr disks. MALDI-TOF-MS spectra were determined on a Bruker REFLEX III instrument equipped with a nitrogen laser operating at 337 nm. NMR spectra were recorded with a Bruker AC-300 instrument. UV/vis spectra were recorded with a Hewlett-Packard 8453 instrument. Transmission electron microscopy (TEM) images were obtained on a JEOL JEM1010 (100 kV) system equipped with a Gatan Bioscan camera for digital imaging. Thermogravimetric analyses (TGA) were recorded on a TA TGQ500 analyzer under nitrogen using Hi-Res Dynamic method (scans, 50 °C/min; resolution setting, 4). Raman spectra were taken at room temperature with a Renishaw Ramascope 2000 microspectrometer and an argon ion laser operating at a wavelength of 514.5 nm as the excitation source. Photophysics: Femtosecond transient absorption studies were performed with 660 nm laser pulses (1 kHz, 150 fs pulse width) from an amplified Ti:Sapphire laser system (Clark-MXR, Inc.). Nanosecond laser flash photolysis experiments were performed with 532 nm laser pulses from a Nd:YAG laser (5 ns pulse width) in a front face excitation geometry. Fluorescence lifetimes were measured with a Laser Strope fluorescence lifetime spectrometer (Photon Technology International) with 337 nm laser pulses from a nitrogen laser fiber-coupled to a lens-based T-formal sample compartment equipped with a stroboscopic detector. Details of the Laser Strobe systems are described on the manufacturer's web site. Emission spectra were recorded by using a FluoroMax-3 (Horiba Co.). The experiments were performed at 20 °C.

2,3,9,10,16,17-Hexa-*tert*-butylphenoxy-23-hydroxymethylphthalocyaninate Zn(II) (1). A mixture of 4-hydroxymethylphthalonitrile[18] (0.20 g, 1.25 mmol), 4,5-*tert*-butylphenoxyphthalonitrile[31] (1.60 g, 3.75 mmol), and $Zn(OAc)_2$ (0.30 g, 1.60 mmol) was refluxed in *N*,*N*-dimethylaminoethanol (10 mL) for 18 h under argon atmosphere. After cooling, the solvent was evaporated, and a mixture of methanol/water (3:1) was added to the residue. The green solid was filtered, washed with methanol, and then subjected to column chromatography on silica gel using $CHCl_3$ as eluent. Trituration with hot methanol yielded 0.21 (11%) of phthalocyanine **1**. mp > 300 °C. ^{1}H NMR (500 MHz, $C_2D_4Cl_4$, 25 °C, TMS): δ = 8.7−8.3 (m, 7H, arom H), 7.4−7.0 (m, 24H, phenyl H), 6.9 (bs, 2H, arom H), 4.7 (bs, 2H, CH_2O), 3.0 (bs, 1H, OH), 1.4−1.2 (m, 54H, $C(CH_3)_3$) ppm. ^{1}H NMR (500 MHz, $C_2D_4Cl_4$, 90 °C, TMS): δ = 8.60−8.20 (m, 7H, arom H), 7.64 (s, 2H, arom H), 7.35, 7.15 (2xm, 24H, phenyl H), 4.83 (s, 2H, CH_2O), 3.09 (s, 1H, OH), 1.30 (m, 54H, $C(CH_3)_3$) ppm. IR (KBr): ν = 2960, 2903, 2867 (CH), 1603 (C═N), 1508, 1488, 1452, 1269, 1216, 1177, 1090, 1029, 893, 828, 744, 722 cm^{-1}; UV/vis ($CHCl_3$): λ_{max} (log ϵ) 355 (4.9), 614 (4.6), 653 (4.5), 680 nm (5.4). MALDI-TOF MS: m/z = 1495 $[M + H]^+$, 1494 $[M^+]$. Anal. Calcd for $C_{93}H_{90}N_8O_7Zn \cdot 2H_2O$: C, 72.85; H, 6.18; N, 7.31. Found: C, 72.24; H, 6.27; N, 7.09.

2,3,9,10,16,17-Hexa-*tert*-butylphenoxy-23-(4-formylbenzoyloxymethyl)phthalocyaninate Zn(II) (2). 4-Formylbenzoic acid (0.010 g, 0.067 mmol), dicyclohexylcarbodiimide (0.013 g, 0.067 mmol), and dimethylaminopyridine (0.008 g, 0.067 mmol) were dissolved in dry THF (5 mL) under argon atmosphere. The solution was cooled to 0 °C in an ice bath and stirred for 20 m. Next, a solution of phthalocyanine **1** (0.1 g, 0.0067 mmol) in 5 mL of dry THF was added dropwise. The mixture was stirred for 1 h at room temperature and for 24 h at room temperature. The resulting reaction crude was filtered through a glass frit to remove the insoluble urea byproduct, and the filtrate was then evaporated and washed with water and methanol. The solid residue was purified by column chromatography in silica gel (hexane/THF, 2:1) to give 0.1 g (93%) of **2**. mp > 300 °C. ^{1}H NMR (300 MHz, $CDCl_3$, 25 °C, TMS): δ = 10.02 (s, 1H, CHO), 8.90 (m, 2H, arom H), 8.70−8.55 (m, 6H, arom H), 8.26 (AA′BB′, 2H), 7.95 (m, 1H, arom H), 7.32, 7.12 (2xm, 24H, phenyl H), 5.78 (s, 2H, CH_2O), 1.40−1.20 (m, 54H, $C(CH_3)_3$) ppm. IR (KBr): ν = 2960, 2903, 2866 (CH), 1727 (COO), 1709 (CHO), 1604 (C═N), 1508, 1489, 1452, 1402, 1269, 1216, 1177, 1090, 1029, 935, 828, 759, 722 cm^{-1}. UV/vis (THF): λ_{max} (log ϵ) 355 (4.84), 614 (4.47), 656 (4.48), 680 nm (5.34). MALDI-TOF MS: m/z = 1627 $[M + H]^+$, 1626 $[M^+]$. Anal. Calcd for $C_{101}H_{94}N_8O_9Zn \cdot H_2O$: C, 73.64; H, 5.87; N, 6.80. Found: C, 73.49; H, 5.88; N, 6.98.

COOH-SWNT. Purified HiPco nanotubes (0.04 g) were sonicated for 15 min in *o*-DCB (40 mL). 4-Formylbenzoic acid (0.64 g) was added to the suspension, and the mixture was heated at 180 °C. *N*-Octylglycine (0.80 g) was added in portions (4 × 0.20 g every 24 h), and the reaction was stopped after 5 days. The crude was filtered

(36) Vázquez, E.; Georgakilas, V.; Prato, M. *Chem. Commun.* **2002**, 2308.

over a PTFE membrane to separate the carbon-based material, which was subsequently sonicated in DMF and centrifugated. The supernatant was separated, the solvent evaporated, and the solid residue was washed consecutively with $CHCl_3$, ethyl acetate, acetone, acetonitrile, methanol, and diethyl ether to give 0.026 g of **COOH-SWNTs**. The concentration of carboxylic acid groups was determined by acid−base titration.[33] **COOH-SWNTs** (5 mg) were stirred in 10 mL of 5×10^{-4} M aqueous NaOH solution under argon for 48 h. The mixture was filtered over a PTFE membrane, and the solid residue was washed with deionized water until the filtrate was neutral. The combined filtrate and washings were titrated with 7.3 mL of 5×10^{-4} M aqueous HCl solution to reach pH 7.0, as monitored by a pH meter. The estimated weight ratio of organic addenda in this material was ca. 7% (1.35×10^{-3} mmol).

ZnPc-SWNT-(1). To a stirred solution of phthalocyanine **1** (26 mg, 0.017 mmol) and EDC (2.7 mg, 0.017 mmol) in THF (10 mL) under argon atmosphere was added HOBT (2.3 mg, 0.017 mmol). Subsequently, a suspension of **COOH-SWNTs** (20 mg) in dry DMF (8 mL) was added, and the resulting mixture was stirred for 4 days. The crude was filtered off, and the black solid was washed with several portions of water, acetone, methanol, ethyl acetate, and THF to give 24 mg of **ZnPc-SWNT-(1)**.

ZnPc-SWNT-(2). Purified HiPco nanotubes (20 mg) were sonicated for 15 min in *o*-DCB (40 mL). Phthalocyanine **2** (26 mg) and *N*-octylglycine (6 mg) were added to the suspension, and the mixture was heated at 180 °C. Sucessive portions of **2** (3×26 mg every 24 h) and *N*-octylglycine (3×6 mg every 24 h) were added, and the reaction was stopped after 5 days. The mixture was filtered over a PTFE membrane, and the black solid was washed with *o*-DCB and subsequently sonicated in DMF and centrifugated. The supernatant was separated, the solvent evaporated, and the solid residue was washed with ethyl acetate, acetonitrile, and methanol, to give 16 mg of **ZnPc-SWNT-2** was collected.

Acknowledgment. We are grateful for financial support from the Ministerio de Educación y Ciencia (CTQ-2005-08933-BQU), Comunidad de Madrid (S-0505/PPQ/000225), and the ESF/MEC (SOHYDS), SFB 583, DFG (GU 517/4-1), FCI and the Office of Basic Energy Sciences of the U.S. Department of Energy (NDRL 4716). We would also like to thank Dr. Eva M. Maya for TGA analyses.

Supporting Information Available: Absorption and fluorescence spectra of **1** titrated with variable concentrations of SWNT; absolute spectra of **ZnPc-SWNT-(2)** in the ground and reduced states; differential absorption spectra of **ZnPc-SWNT-(2)** in the visible and NIR upon femtosecond flash photolysis (660 nm) and their time−absorption profiles at different wavelengths; differential absorption spectra of **ZnPc-SWNT-(1)** in the visible and NIR upon femtosecond flash photolysis (660 nm); and full Raman spectra of pristine and functionalized nanotubes. This material is available free of charge via the Internet at http://pubs.acs.org.

JA068240N